

Pilot Application of Magnetic Nanoparticle-Based Biosensor for Necrotizing Enterocolitis

Dokyoon Kim^{1#}, Changlin Fu^{2#}, Xuefeng B Ling^{2#}, Zhongkai Hu², Guozhong Tao², Yingzhen Zhao², Zachary J Kastenberg², Karl G Sylvester^{2*} and Shan X Wang^{1,3*}

¹Department of Materials Science and Engineering, Stanford University, Stanford, CA 94305, USA

²Department of Surgery, Stanford University, Stanford, CA 94305, USA

³Department of Electrical Engineering, Stanford University, Stanford, CA 94305, USA

[#]These authors contributed equally to this work

Abstract

Background: Necrotizing Enterocolitis (NEC) is a major source of neonatal morbidity and mortality. There is an ongoing need for a sensitive diagnostic instrument to discriminate NEC from neonatal sepsis. We hypothesized that magnetic nanoparticle-based biosensor analysis of gut injury-associated biomarkers would provide such an instrument.

Study design: We designed a magnetic multiplexed biosensor platform, allowing the parallel plasma analysis of C-reactive protein (CRP), matrix metalloproteinase-7 (MMP7), and epithelial cell adhesion molecule (EpCAM). Neonatal subjects with sepsis (n=5) or NEC (n=10) were compared to control (n=5) subjects to perform a proof of concept pilot study for the diagnosis of NEC using our ultra-sensitive biosensor platform.

Results: Our multiplexed NEC magnetic nanoparticle-based biosensor platform was robust, ultrasensitive (Limit of detection LOD: CRP 0.6 pg/ml; MMP7 20 pg/ml; and EpCAM 20 pg/ml), and displayed no cross-reactivity among analyte reporting reagents. To gauge the diagnostic performance, bootstrapping procedure (500 runs) was applied: MMP7 and EpCAM collectively differentiated infants with NEC from control infants with ROC AUC of 0.96, and infants with NEC from those with sepsis with ROC AUC of 1.00. The 3-marker panel comprising of EpCAM, MMP7 and CRP had a corresponding ROC AUC of 0.956 and 0.975, respectively.

Conclusion: The exploration of the multiplexed nano-biosensor platform shows promise to deliver an ultrasensitive instrument for the diagnosis of NEC in the clinical setting.

Keywords: Necrotizing enterocolitis; NEC; Diagnosis; Sepsis; Nanoparticle; Biosensor

Introduction

Necrotizing enterocolitis (NEC) is one of the most common life-threatening diseases of the newborn. NEC predominantly affects low birth weight infants in the first weeks of life with a reported frequency of between 1% and 5% of NICU admissions [1,2] and mortality rates for infants with NEC ranging from 15% to 30%. The pathogenesis of NEC includes progressive inflammation of the gut involving enteric bacteria, the innate immune system, and a compromised intestinal epithelial barrier resulting in eventual necrosis in advanced cases.

Approximately one half of all infants with NEC have mild disease that will recover with medical therapy (medical NEC) [3,4]. This mild form of the disease is very similar to neonatal sepsis. The remaining patients progress to intestinal gangrene with perforation and/or irreversible necrosis requiring emergency surgical intervention (surgical NEC). Several studies have demonstrated that surgical intervention for NEC is an independent risk factor for long-term growth abnormalities, adverse neurodevelopmental outcomes, and gastrointestinal morbidity including short bowel syndrome [3,4]. Improvement in NEC outcomes will require the development of sensitive and specific diagnostic instruments to discriminate NEC from sepsis to enable further study of new medical and surgical therapies as they are developed [5].

C-reactive protein (CRP) is an acute-phase protein whose levels rise in response to inflammation. In infants with inflammatory conditions including NEC, persistently elevated CRP is often used as an indication to both begin and continue medical therapy, often including

antibiotics. It is however also widely recognized that CRP is a non-specific indicator of neonatal sepsis [6-8]. There is a need for a novel set of NEC-specific biomarkers that can be analyzed in a multiplex format over a broad dynamic range of possible analyte concentrations. An additional improvement upon existing technology would be an assay with a detection limit that exceeds currently available immune-based detection platforms.

There have been numerous recent attempts to identify candidate markers of gut injury that discriminate NEC from other inflammatory conditions [4,9-13]. Significant elevations in the measured plasma levels of Platelet Activating Factor (PAF) [14,15], inter-alpha inhibitor protein [16], calprotectin, claudin [13], intestinal fatty acid binding protein (iFABP) [17], and C-reactive protein (CRP) [18] have all been associated with the onset of NEC. While several of these (calprotectin and iFABP) have been described in other intestinal diseases, others are

***Corresponding authors:** Karl G Sylvester, Department of Surgery, Stanford University, Stanford, CA 94305, USA, E-mail: karls@stanford.edu

Shan X Wang, Department of Electrical Engineering, Stanford University, Stanford, CA 94305, USA, Tel: (650)-427-9198; Fax: (650)-723-1154; E-mail: sxwang@stanford.edu

Received November 05, 2013; **Accepted** December 16, 2013; **Published** December 18, 2013

Citation: Kim D, Fu C, Ling XB, Hu Z, Tao G, et al. (2013) Pilot Application of Magnetic Nanoparticle-Based Biosensor for Necrotizing Enterocolitis. J Proteomics Bioinform S5: 002. doi:[10.4172/jpb.S5-002](http://dx.doi.org/10.4172/jpb.S5-002)

Copyright: © 2013 Kim D, et al. This is an open-access article distributed under the terms of the Creative Commons Attribution License, which permits unrestricted use, distribution, and reproduction in any medium, provided the original author and source are credited.

non-specific markers of inflammation (PAF and CRP). Importantly, other than CRP, none have been widely adopted in clinical practice. Importantly, most of these target analytes were measured in isolation, not in combination. Given the high biologic variability and heterogeneous nature of NEC, we reasoned that a multiplex analyte detection scheme would provide greater flexibility in a clinical setting.

The candidate diagnostic biomarkers, EpCAM and MMP7, were targeted based upon their known biologic significance and previous studies suggesting their possible association with NEC and other gut pathology. Matrix metalloproteinase 7 (MMP7) has been proposed to play a role in NEC associated tissue injury and inflammation due to its involvement in tissue remodeling and cell migration [19]. Epithelial cell adhesion molecule (EpCAM) is a transmembrane glycoprotein, which is expressed exclusively in epithelia, therefore, a potential tissue destruction biomarker. In addition, the upregulation of EpCAM expression on epithelial cells observed during inflammatory processes [20,21] suggests a role of EpCAM in regeneration after tissue damage, i.e. cell proliferation and differentiation. Furthermore, in order to investigate the performance characteristics of the magnetic-nanoparticle (MNP) platform, the availability of reliable immune-reagents for these analytes was an additional technical consideration in designing this pilot study.

Recent advances in biosensor technologies for *in vitro* diagnostics provide the potential to transform the practice of medicine. We previously described a MNP based multiplex protein detection platform able to detect a constellation of biomolecules in diverse clinical samples (for example, serum, urine, cell lysates or saliva) with high sensitivity (down to attomolar resolution) and large linear dynamic range (more than four decades) [22,23]. The multianalyte ability, sensitivity, scalability, and ease of use of the MNP-based protein assay technology make it a strong candidate platform for versatile molecular diagnostics in both research and clinical settings. We postulated that the integration of our MNP technology with CRP, MMP-7, and EpCAM would provide a platform for the development of a diagnostic instrument for the gut specific pediatric disease NEC.

Methods

Ethics and sample collection

Informed consent was obtained from the parents of all enrolled subjects. This study was approved by the human subjects protection programs at each participating institution (Yale-New Haven Children's Hospital, Lucile Packard Children's Hospital at Stanford University, and the Children's Hospital of Philadelphia). Blood samples were collected and plasma was isolated by centrifuging the collected blood, and stored at -80°C prior to analysis.

Reagents

Anti-human CRP antibody (R&D systems, MAB17071), biotinylated anti-human CRP antibody (R&D systems, BAM17072), native human CRP protein (Biospecific, J81600), anti-human MMP7 antibody (R&D systems, MAB9072), biotinylated anti-human MMP7 antibody (R&D systems, BAF2907), recombinant human MMP7 protein (R&D systems, 907-MP-010), anti-human EpCAM antibody (BioMab, EpAb3-5), biotinylated anti-human EpCAM antibody (R&D systems, MAB9601), recombinant human EpCAM protein (R&D systems, 960-EP-050), poly(allylamine hydrochloride) (Polyscience, 71550-12-4), poly(ethylene-alt-maleic anhydride) (Aldrich, 188050), 1x phosphate buffered saline (PBS) (Invitrogen), 1-ethyl-3-(3-

dimethylaminopropyl)carbodiimide hydrochloride (EDC) (Thermo scientific), N-hydroxysuccinimide (NHS) (Aldrich), 1% bovine serum albumin (BSA) (Aldrich), biotinylated bovine serum albumin (biotin-BSA) (Pierce), Tween 20 (Aldrich), and streptavidin-coated MicroBeads (Miltenyi, 130-048-101) were used as received and without further purification.

Magnetic protein chip surface preparation

The magnetic protein chip was fabricated by previously reported method [22,23]. The chip surface was washed with acetone, methanol, and isopropanol. Subsequently, the surface was further cleaned by exposing to oxygen plasma (Harrick Plasma, PDC-32G) for 3 minutes. Then, the surface was immersed in a 1% aqueous solution of poly(allylamine hydrochloride) for 5 minutes, followed by rinsing with deionized water. The magnetic protein chip was baked at 120°C for 1 hour. After incubation in a 2% aqueous solution of poly(ethylene-alt-maleic anhydride), the surface was washed again with deionized water and activated by adding a mixture of 1-ethyl-3-[3-dimethylaminopropyl] carbodiimide hydrochloride and N-hydroxysuccinimide in deionized water. A robotic spotter (Scienion, sciFlexarrayer) was then used to deposit capture antibody solution on the magnetic protein chip surface. PBS solutions of anti-human CRP (0.5 mg/ml), anti-human MMP7 (0.5 mg/ml), and anti-human EpCAM (0.5 mg/ml) were deposited on at least 10 sensors on the magnetic protein chip for each solution. Also, 0.1% PBS solutions of BSA and biotin-BSA were placed over 10 sensors as negative and positive controls, respectively. Reference sensors for measurement of electrical background signals were covered with thick silicon oxide to isolate them from surface reactions. Finally, the prepared magnetic protein chip was stored in a humidity chamber at 4°C before use.

CRP assay protocol

After washing the magnetic protein chip surface with a washing buffer (0.1% BSA and 0.05% Tween 20 in PBS), the surface was blocked with 1% BSA for 1 hour to avoid unwanted adhesion of non-specific biomolecules. Then, the surface was washed again and immersed in a 10000× diluted plasma sample (diluted in dilution buffer, 0.1% BSA and 0.05% Tween 20 in PBS) for 2 hours. The sample solution was washed away using the washing buffer, and a biotinylated anti-human CRP antibody solution with a concentration of 5 µg/ml was added. Following 1 hour incubation with the biotinylated anti-human CRP antibody, the surface was washed again using the washing buffer before measuring CRP signals from the chip. Real-time signals were collected using a custom designed electric read-out system. Briefly, streptavidin-coated magnetic nanoparticles (Miltenyi, streptavidin MicroBeads) were added to the prepared magnetic protein chip to induce an analyte concentration-dependent signal change. The observed signals were converted to corresponding concentrations using standard curves for each biomarker.

MMP7/EpCAM duplex-assay protocol

Similar procedures as those used in CRP assay were used for the duplex measurement of MMP7 and EpCAM, except that 2× diluted plasma samples and a mixture of biotinylated anti-human MMP7 antibody and biotinylated anti-human EpCAM antibody solutions (final concentration of 5 µg/ml for each antibody) were used.

Statistical data analysis

Patient demographic data was analyzed using the "Epidemiological

calculator” (R epicalc package). Student’s t test was performed to calculate *p* values for continuous variables, and Fisher exact test was used for comparative analysis of categorical variables. Hypothesis testing was performed using Student’s t-test (two tailed) and Mann-Whitney U-test (two tailed). The biomarker panel score was defined as the ratio between the geometric means of the respective up- and down-regulated protein biomarkers, and was evaluated by ROC curve analysis [24,25]. 500 testing data sets, generated by bootstrapping, from the biosensor data were used to derive estimates of standard errors and confidence intervals for our ROC analysis. The plotted ROC curve is the vertical average of the 500 bootstrapping runs, and the box and whisker plots show the vertical spread around the average.

Results

Demographics

In our cohort (Table 1, NEC n=10; sepsis n=5; control n=5), gender, race, gestational age and birth weight, length and head circumference related differences were analyzed between different subject groups. Statistical differences (*p*-value:<0.05) were observed in birth weight, birth length, and birth head circumference among the three groups. No statistical differences were observed in gender, race and gestation age.

Magnetic protein chip calibration of human CRP, MMp7, and EpCAM

We prepared standard curves to calibrate the magnetic protein chip measurements of CRP, MMp7, and EpCAM in plasma samples (Figure 1). The standard curves were generated from measurements where each protein was spiked in various concentrations into PBS. The standard dilutions of plasma samples (10,000× for CRP and 2× for MMp7 and EpCAM, respectively) were chosen so that all measured signals were within the linear dynamic range of the standard curve for each protein. We did not observe any cross-reactivity between the reagents used in this study, which was confirmed by the fact that experiments with several mixture combinations of different target proteins and different antibodies did not show any difference in their signals.

The CRP standard curve measured on the magnetic protein chips had a linear dynamic range of more than three orders of magnitude (0.6 ~3,000 pg/ml) with an *R*² value of 0.97 (Figure 1A). Our magnetic protein chip immunoassay had a detection limit for CRP (0.6 pg/ml) that was lower than currently available commercial ELISA kits (range, generally ~2 to ~15 pg/ml) or other multiplex assay platforms such as Luminex and Mesoscale (range, 1.4 to 2 pg/ml for Luminex and 100 pg/ml for Mesoscale). The upper limit of the linear dynamic range for CRP (3,000 pg/ml) was higher than that of ELISA (~1,000 pg/ml), was similar to that of Luminex (range, 2,000 to 8,000 pg/ml), but was lower than that of Mesoscale (400,000 pg/ml).

The magnetic protein chips showed an MMp7 standard curve covering about four orders of magnitude as its linear dynamic range (10 ~ 100,000 pg/ml) with an *R*² value of >0.99 (Figure 1B). The detection limit of MMp7 magnetic protein chip immunoassay was 20 pg/ml, which was lower than that of ELISA (range, generally ~30 to ~150 pg/ml), but was higher than that of Luminex (4 pg/ml). The upper limits of the linear dynamic range for MMp7 were similar for magnetic protein chips, ELISA, and Luminex (100 ng/ml for magnetic protein chips, ranges from 2 to 100 ng/ml for ELISA, and 60 ng/ml for Luminex). A Mesoscale kit for MMp7 was not available commercially at the time of this study.

Figure 1C shows the standard curve for EpCAM measured on the magnetic protein chips. It has a linear dynamic range of more than three orders of magnitude (20 ~ 50,000 pg/ml) with an *R*² value of 0.96. The detection limit of EpCAM magnetic protein chip immunoassay (20 pg/ml) was lower than that of ELISA (range, generally ~20 to ~50 pg/ml), but was comparable to that of Luminex (13.7 pg/ml). The upper limit of the linear dynamic range was highest for the magnetic protein chips (50,000 pg/ml) compared with ELISA (range, ~6,000 to ~12,000 pg/ml).

CRP, MMp7, and EpCAM concentrations in plasma of NEC, sepsis, and healthy control infants

Using the standard curves shown in Figure 1, we tested the ability of our magnetic protein chip platform to detect the concentration differences of CRP, MMp7, and EpCAM in blood plasma collected from infants with NEC, infants with sepsis, and healthy infants. We performed the immunoassay using two magnetic protein chips per plasma sample, one for CRP assay, and the other for duplex assay of MMp7 and EpCAM.

As shown in Figure 2A, the concentrations of CRP were 4.6 ± 5.0 µg/ml (range, ~0 to 14.2) in the NEC, 0.5 ± 1.0 µg/ml (range, ~0 to 2.2) in the sepsis, and 0.1 ± 0.2 µg/ml (range, ~0 to 0.4) in the healthy control samples. Although the average concentration of CRP was much higher in the NEC samples than in the sepsis or healthy control samples, there were five and three NEC samples whose CRP concentrations were within the CRP concentration range of the sepsis and healthy control samples, respectively. The concentrations of MMp7 (Figure 2B) were 18.0 ± 10.5 ng/ml (range, ~4.3 to 36.1) in the NEC, 82.0 ± 13.2 ng/ml (range, ~72.1 to 103.3) in the sepsis, and 82.0 ± 40.5 ng/ml (range, ~17.8 to 118.8) in the healthy control samples. The average concentration of MMp7 in the NEC samples was four times less than

Characteristic	NEC (n=10)	Sepsis (n=5)	Control (n=5)	<i>p</i> -value
Gender				1
Female	4(40%)	2(40%)	2(40%)	
Male	6(60%)	3(60%)	3(60%)	
Race				0.418
Asian	3(30%)	0(0%)	2(40%)	
Black	2(20%)	0(0%)	0(0%)	
White	5(50%)	5(100%)	3(60%)	
Gestation age (weeks)				0.078
Median	26.5	26	34	
(IQR)	(24.0, 31.0)	(26, 29)	(33, 35)	
Birth weight (grams)				0.028*
Median	810	950	2560	
(IQR)	(680, 1050)	(710, 1180)	(1900, 2820)	
Birth length (cm)				0.042*
Median	33	36.5	44	
(IQR)	(32, 35)	(32.0, 37.0)	(42.75, 46.00)	
Birth head circumference (cm)				0.042*
Median	23.75	25.5	33	
(IQR)	(22.00, 29.00)	(23.0, 26.5)	(31.250, 33.125)	

IQR, interquartile range. **p*-value<0.05

Table 1: Patient demographics.

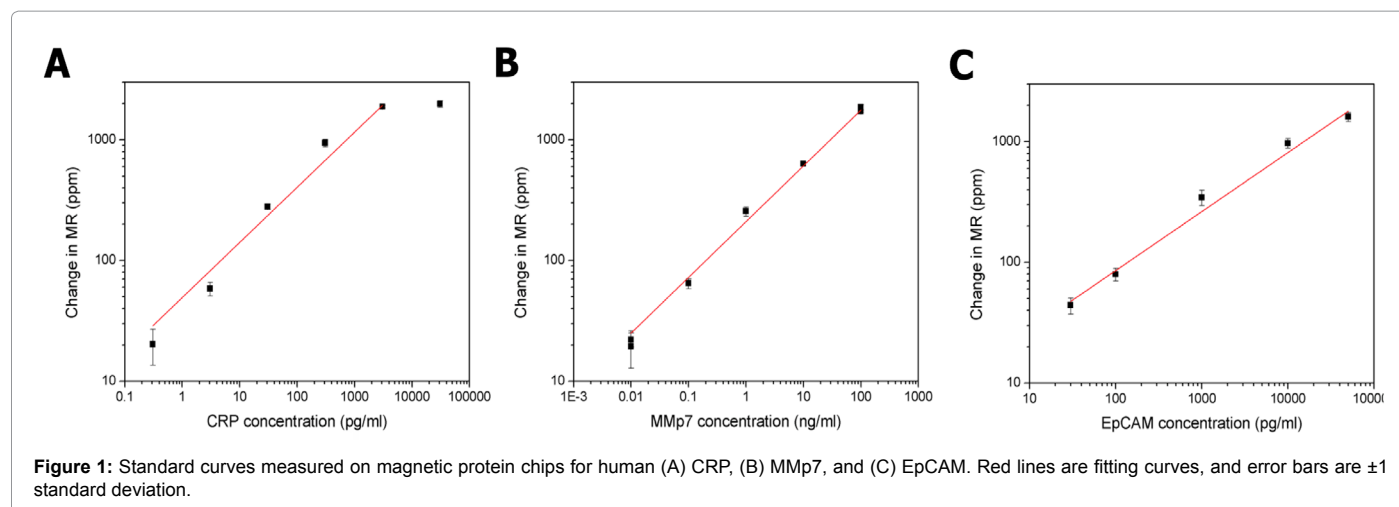


Figure 1: Standard curves measured on magnetic protein chips for human (A) CRP, (B) MMP7, and (C) EpCAM. Red lines are fitting curves, and error bars are ± 1 standard deviation.

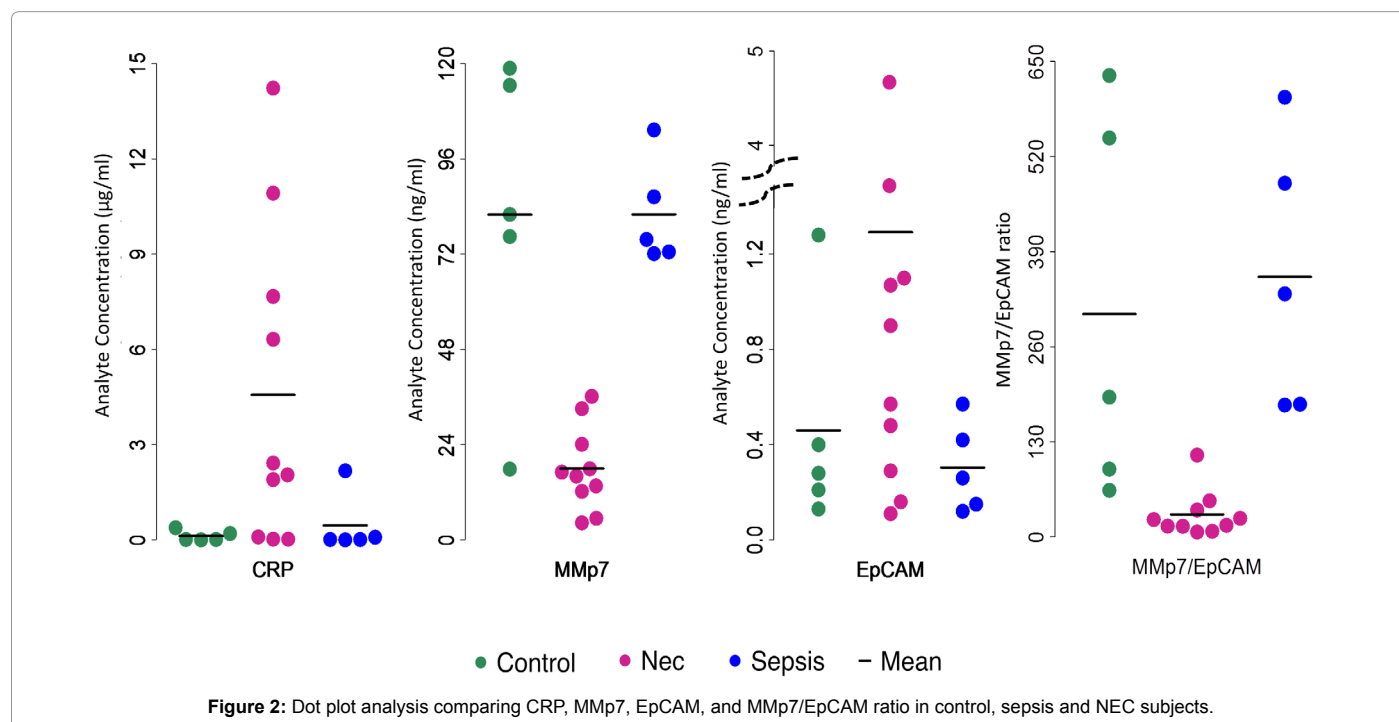


Figure 2: Dot plot analysis comparing CRP, MMP7, EpCAM, and MMP7/EpCAM ratio in control, sepsis and NEC subjects.

that of the sepsis or healthy control samples, and the concentration range of the NEC samples was relatively well separated from those of the sepsis and healthy control samples. The concentrations of EpCAM (Figure 2C) were 1.3 ± 1.6 ng/ml (range, ~ 0.1 to 4.7), 0.3 ± 0.2 ng/ml (range, ~ 0.1 to 0.6), and 0.5 ± 0.5 ng/ml (range, ~ 0.1 to 1.3) in the NEC, sepsis, and healthy control samples, respectively. The higher average concentration of EpCAM observed for the NEC samples was mainly due to two samples which showed about 7-fold higher concentrations than the remainder of the NEC samples. The concentration of EpCAM in the NEC samples after excluding those two samples was 0.6 ± 0.4 ng/ml (range ~ 0.1 to 1.1), which is similar to those of sepsis or healthy control samples.

Table 2 lists the p values calculated using Mann-Whitney U test. The CRP concentrations in the NEC samples were significantly different from those of the sepsis or healthy control samples ($p < 0.05$).

However, CRP concentration difference between sepsis and healthy control samples was not significant ($p = 1.0000$). MMP7 also showed a significant concentration difference between NEC samples and sepsis samples, and between NEC samples and healthy control samples ($p < 0.05$). Again, however, MMP7 concentration difference between sepsis and healthy control samples was not significant ($p = 0.4647$). EpCAM did not show significant concentration difference (p value > 0.05) among the sample groups.

A panel of MMP7 and EpCAM to discriminate NEC and sepsis

Using MNP biosensor data, we constructed a panel of MMP7 and EpCAM, and the ratio of the two analytes was tested in assessing NEC and sepsis (Figure 2D). The MMP7/EpCAM ratio's NEC and sepsis discriminant utility was demonstrated in this study (NEC vs. control, ROC AUC 0.963; NEC vs. sepsis, ROC AUC 1.00). Other possible

panel constructions, including CRP/EpCAM ratio (Supplementary Figure 1, NEC vs. control, ROC AUC 0.882; NEC vs. sepsis, ROC AUC 0.901) or combining CRP, MMp7 and EpCAM (Supplementary Figure 2, NEC vs. control, ROC AUC 0.956; NEC vs. sepsis, ROC AUC 0.975), were also evaluated. However, MMp7/EpCAM ratio was demonstrated to be the best panel in regard to the discrimination of NEC, sepsis and control subjects (Figure 3).

Discussion

The clinical presentation of NEC is very similar to that of neonatal sepsis and there are no reliable diagnostic instruments to aid in discriminating these conditions. Clinicians have therefore utilized combinations of non-specific clinical and laboratory indicators to guide patient management. NEC is ultimately diagnosed through a combination of clinical, radiographic, and laboratory findings that in aggregate define the original diagnostic Bell's criteria. This study tested the hypothesis that gut injury and remodeling associated proteins (CRP, MMp7, and EpCAM) could be multiplexed on an ultrasensitive and matrix insensitive biosensor platform to aid in the diagnosis of NEC. ROC curve analysis demonstrated that the MMp7/EpCAM ratio maintains robust performance characteristics. This is encouraging and further suggests an additional advantage of this type of ultrasensitive biosensor platform, which has the capacity to stratify low concentration biomarkers for categorical diagnostic discrimination and may allow early disease state detection.

We recognize several limitations to this proof of concept study. The small sample size limits our ability to validate statistically significant associations, but the overall sensitivity of the biosensor platform is encouraging for future clinical utility. To gauge the diagnostic performance of our nano-biosensor, we performed a simulation analysis with 500 bootstrapping runs and subsequent ROC analyses. Bootstrapping can be a very useful tool in statistics. However, we should proceed with caution when interpreting the promising results from this exploratory analysis with a small sample size. Power analysis

Analyte	Nec vs. Control	Nec vs. Sepsis	Sepsis vs. Control
CRP (pg/ml)	0.023218*	0.031782*	1.00000
MMp7 (ng/ml)	0.007992	0.000666**	0.547619
EpCAM(ng/ml)	0.309603	0.111027	0.841270

*p<0.05; ** p<0.005

Table 2: Comparative analysis of the plasma abundance between disease categories.

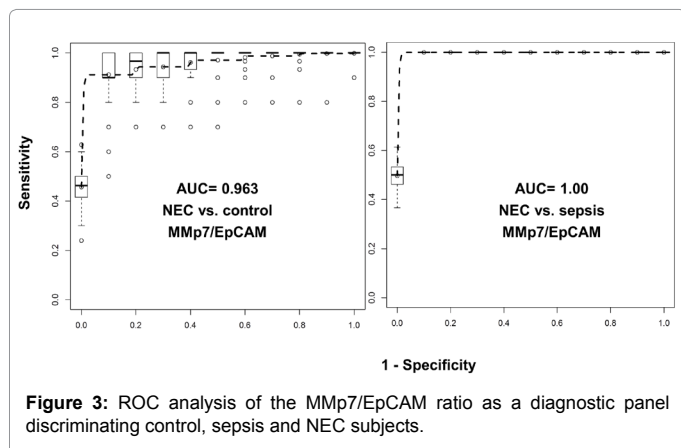


Figure 3: ROC analysis of the MMp7/EpCAM ratio as a diagnostic panel discriminating control, sepsis and NEC subjects.

should be applied to guide the assembly of the future sample cohort to validate our pilot study results with sufficient power.

A second limitation of our study was the lack of longitudinal sampling of subjects with suspected NEC and sepsis. Given that our biosensor platform is ultrasensitive, the biosensor may be able to assess impending NEC and sepsis in a sub-clinical stage. In addition, serial sampling would also provide greater understanding of the variability of the measured analytes relative to disease onset and progression. While a large proportion of the controls were referred to our neonatal intensive care unit for evaluation of possible NEC and sepsis, this was not uniformly true as some controls likely had a low pre-test probability of NEC or sepsis. Since the pre-test probability is an important consideration in evaluating the performance of a diagnostic test, collection of this information will be critical in the next testing phase of our biosensor diagnostic test.

In this study, all babies with NEC had the pathognomonic abdominal radiographic finding of pneumatosis intestinale, and all babies with sepsis had culture positive findings. Among our sepsis patients we observed the absence of uniform serum CRP elevation, a finding consistent with the heterogeneity of sepsis and the variability of correlative elevations in CRP [6-8].

In addition to larger prospective validation of the results reported here, we intended to construct a model that integrated the biosensor quantifications with clinical, radiographic, and laboratory findings to prospectively identify infants with NEC. We anticipate that a larger prospective trial of the MMp7/EpCAM biosensor algorithm with integrated analysis of readily available existing clinical parameters will lead to a robust instrument that can be run routinely in the hospital setting for neonatal care of sepsis and NEC. It is our hope that the future integration of diagnostic biosensor platforms into clinical practice will facilitate iterative patient sample testing to guide treatment strategies throughout the course of disease progression and recovery.

Acknowledgements

The authors would like to acknowledge the following individuals who contributed samples from their institutions for this study: Dr. Richard Ehrenkranz (Yale New Haven) and Dr. Mary Cay Harris (CHOP). The authors would like to thank Drs. Harvey Cohen and John Whittin for critical discussions, which greatly improve the quality of the paper. This work was in part supported by Stanford's Bio-X seed grant (to KGS, SXW and XBL). The work at Stanford also benefited from the National Cancer Institute grants Center for Cancer Nanotechnology Excellence (U54CA151459) and Physical Science Oncology Center (U54CA143907).

Conflict of Interest

S.X.W. holds patents on magnetic biosensors that are assigned to Stanford University and out-licensed to MagArray Inc. for commercialization. He is also a scientific founder of the startup company and owns stock equity.

References

- Guthrie SO, Gordon PV, Thomas V, Thorp JA, Peabody J, et al. (2003) Necrotizing enterocolitis among neonates in the United States. *J Perinatol* 23: 278-285.
- Kamitsuka MD, Horton MK, Williams MA (2000) The incidence of necrotizing enterocolitis after introducing standardized feeding schedules for infants between 1250 and 2500 grams and less than 35 weeks of gestation. *Pediatrics* 105: 379-384.
- Blakely ML, Tyson JE, Lally KP, McDonald S, Stoll BJ, et al. (2006) Laparotomy versus peritoneal drainage for necrotizing enterocolitis or isolated intestinal perforation in extremely low birth weight infants: outcomes through 18 months adjusted age. *Pediatrics* 117: e680-e687.
- Hintz SR, Kendrick DE, Stoll BJ, Vohr BR, Fanaroff AA, et al. (2005) Neurodevelopmental and growth outcomes of extremely low birth weight infants after necrotizing enterocolitis. *Pediatrics* 115: 696-703.

5. Lin PW, Stoll BJ (2006) Necrotizing enterocolitis. *Lancet* 368: 1271-1283.
6. Pourcyrous M, Korones SB, Yang W, Boulden TF, Bada HS (2005) C-reactive protein in the diagnosis, management, and prognosis of neonatal necrotizing enterocolitis. *Pediatrics* 116: 1064-1069.
7. Cetinkaya M, Ozkan H, Köksal N, Akaci O, Özgür T (2011) Comparison of the efficacy of serum amyloid A, C-reactive protein, and procalcitonin in the diagnosis and follow-up of necrotizing enterocolitis in premature infants. *J Pediatr Surg* 46: 1482-1489.
8. Póvoa P, Almeida E, Moreira P, Fernandes A, Mealha R, et al. (1998) C-reactive protein as an indicator of sepsis. *Intensive Care Med* 24: 1052-1056.
9. Derikx JP, Evennett NJ, Degraeuwe PL, Mulder TL, van Bijnen AA, et al. (2007) Urine based detection of intestinal mucosal cell damage in neonates with suspected necrotizing enterocolitis. *Gut* 56: 1473-1475.
10. Guthmann F, Borchers T, Wolfrum C, Wustrack T, Bartholomäus S, et al. (2002) Plasma concentration of intestinal- and liver-FABP in neonates suffering from necrotizing enterocolitis and in healthy preterm neonates. *Mol Cell Biochem* 239: 227-234.
11. Sylvester KG, Ling XB, Liu GY, Kastenber ZJ, Ji J, et al. (2013) A novel urine peptide biomarker-based algorithm for the prognosis of necrotizing enterocolitis in human infants. *Gut* .
12. Sylvester KG, Ling XB, Liu GY, Kastenber ZJ, Ji J, et al. (2013) A novel urine peptide biomarker-based algorithm for the prognosis of necrotizing enterocolitis in human infants. *Gut* .
13. Thuijls G, Derikx JP, van Wijck K, Zimmermann LJ, Degraeuwe PL, et al. (2010) Non-invasive markers for early diagnosis and determination of the severity of necrotizing enterocolitis. *Ann Surg* 251: 1174-1180.
14. Rabinowitz SS, Dzakpasu P, Piecuch S, Leblanc P, Valencia G, et al. (2001) Platelet-activating factor in infants at risk for necrotizing enterocolitis. *J Pediatr* 138: 81-86.
15. Young C, Sharma R, Handfield M, Mai V, Neu J (2009) Biomarkers for infants at risk for necrotizing enterocolitis: clues to prevention? *Pediatr Res* 65: 91R-97R.
16. Chaaban H, Shin M, Sirya E, Lim YP, Caplan M, et al. (2010) Inter-alpha inhibitor protein level in neonates predicts necrotizing enterocolitis. *J Pediatr* 157: 757-761.
17. Evennett NJ, Hall NJ, Pierro A, Eaton S (2010) Urinary intestinal fatty acid-binding protein concentration predicts extent of disease in necrotizing enterocolitis. *J Pediatr Surg* 45: 735-740.
18. Pourcyrous M, Bada HS, Korones SB, Baselski V, Wong SP (1993) Significance of serial C-reactive protein responses in neonatal infection and other disorders. *Pediatrics* 92: 431-435.
19. Bister V, Salmela MT, Heikkilä P, Anttila A, Rintala R, et al. (2005) Matrilysins-1 and -2 (MMP-7 and -26) and metalloelastase (MMP-12), unlike MMP-19, are up-regulated in necrotizing enterocolitis. *J Pediatr Gastroenterol Nutr* 40: 60-66.
20. Trzpis M, Popa ER, McLaughlin PM, van Goor H, Timmer A, et al. (2007) Spatial and temporal expression patterns of the epithelial cell adhesion molecule (EpCAM/EGP-2) in developing and adult kidneys. *Nephron Exp Nephrol* 107: e119-131.
21. Trzpis M, McLaughlin PM, de Leij LM, Harmsen MC (2007) Epithelial cell adhesion molecule: more than a carcinoma marker and adhesion molecule. *Am J Pathol* 171: 386-395.
22. Gaster RS, Hall DA, Nielsen CH, Osterfeld SJ, Yu H, et al. (2009) Matrix-insensitive protein assays push the limits of biosensors in medicine. *Nat Med* 15: 1327-1332.
23. Osterfeld SJ, Yu H, Gaster RS, Caramuta S, Xu L, et al. (2008) Multiplex protein assays based on real-time magnetic nanotag sensing. *Proc Natl Acad Sci U S A* 105: 20637-20640.
24. Zweig MH, Campbell G (1993) Receiver-operating characteristic (ROC) plots: a fundamental evaluation tool in clinical medicine. *Clin Chem* 39: 561-577.
25. Sing T, Sander O, Beerenwinkel N, Lengauer T (2005) ROCr: visualizing classifier performance in R. *Bioinformatics* 21: 3940-3941.

Citation: Kim D, Fu C, Ling XB, Hu Z, Tao G, et al. (2013) Pilot Application of Magnetic Nanoparticle-Based Biosensor for Necrotizing Enterocolitis. *J Proteomics Bioinform* S5: 002. doi:[10.4172/jpb.S5-002](https://doi.org/10.4172/jpb.S5-002)

This article was originally published in a special issue, **Proteomics & Biomarker** handled by Editors. Dr. Lifeng Peng, Victoria University of Wellington, New Zealand; Dr. Sreenivasa Rao Ramisetty, Idexx Laboratories, USA